

Pulsed-Laser Deposited Amorphous Diamond and Related Materials: Synthesis, Characterization, and Field Emission Properties

Vladimir I. Merkulov^a, Douglas H. Lowndes^a, L. R. Baylor^b, G. E. Jellison, Jr.^a,
A. A. Puretzky^a, and D. B. Geohegan^a

^a Solid State Division

^b Fusion Energy Division

Oak Ridge National Laboratory, Oak Ridge, TN 37831

Submitted to:

Laser Applications in Microelectronic and Optoelectronic Manufacturing IV

Conference proceedings of SPIE, 1999

"The submitted manuscript has been authored by a contractor of the U.S. Government under contract DE-AC05-96OR22464. Accordingly, the U.S. Government retains a nonexclusive, royalty-free license to publish or reproduce the published form of this contribution, or allow others to do so, for U.S. Government purposes."

RECEIVED

MAR 03 1999

OSTI

Prepared by

Solid State Division

Oak Ridge National Laboratory

P.O. Box 2008

Oak Ridge, Tennessee 37831-6056

managed by

LOCKHEED MARTIN ENERGY RESEARCH CORP.

for the

U.S. DEPARTMENT OF ENERGY

under contract DE-AC05-96OR22464

DISCLAIMER

This report was prepared as an account of work sponsored by an agency of the United States Government. Neither the United States Government nor any agency thereof, nor any of their employees, make any warranty, express or implied, or assumes any legal liability or responsibility for the accuracy, completeness, or usefulness of any information, apparatus, product, or process disclosed, or represents that its use would not infringe privately owned rights. Reference herein to any specific commercial product, process, or service by trade name, trademark, manufacturer, or otherwise does not necessarily constitute or imply its endorsement, recommendation, or favoring by the United States Government or any agency thereof. The views and opinions of authors expressed herein do not necessarily state or reflect those of the United States Government or any agency thereof.

DISCLAIMER

**Portions of this document may be illegible
in electronic image products. Images are
produced from the best available original
document.**

Pulsed-Laser Deposited Amorphous Diamond and Related Materials: Synthesis, Characterization, and Field Emission Properties

Vladimir I. Merkulov^a, Douglas H. Lowndes^a, L. R. Baylor^b, G. E. Jellison, Jr.^a,
A. A. Puretzky^a, and D. B. Geohegan^a.

^a Solid State Division

^b Fusion Energy Division

Oak Ridge National Laboratory, Oak Ridge, TN 37831

ABSTRACT

Amorphous carbon films with variable sp^3 content were produced by ArF (193nm) pulsed laser deposition. An *in-situ* ion probe was used to measure kinetic energy of C^+ ions. In contrast to measurements made as a function of laser fluence, ion probe measurements of kinetic energy are a convenient as well as more accurate and fundamental method for monitoring deposition conditions, with the advantage of being readily transferable for inter-laboratory comparisons. Electron energy loss spectroscopy (EELS) and spectroscopic ellipsometry measurements reveal that tetrahedral amorphous carbon (ta-C) films with the most diamond-like properties are obtained at the C ion kinetic energy of ~ 90 eV. Film properties are uniform within a $12\text{-}15^\circ$ angle from the plume centerline. Tapping-mode atomic force microscope measurements show that films deposited at near-optimum kinetic energy are extremely smooth, with rms roughness of only ~ 1 Å over distances of several hundred nm. Field emission (FE) measurements show that ta-C does not appear to be a good electron emitter. After conditioning of ta-C films deposited on n-type Si a rather high turn-on voltage of ~ 50 V/ μ m was required to draw current of ~ 1 nA to the probe. The emission was unstable and typically ceased after a few minutes of operation. The FE tests of ta-C and other materials strongly suggest that surface morphology plays a dominant role in the FE process, in agreement with conventional Fowler-Nordheim theory.

Keywords: Diamond, tetrahedral amorphous carbon, pulsed laser ablation, EELS, ellipsometry, field emission

1. INTRODUCTION

Hard amorphous carbon films has drawn significant attention of the industrial and scientific communities since the first reports on their deposition more than two decades ago^{1, 2}. More recent studies have focused on hydrogen-free amorphous diamond films (also known as tetrahedral amorphous carbon, ta-C) that have superior diamond-like properties^{3, 4}, such as high hardness, a large (~ 2 eV) optical (Tauc) band gap and a low coefficient of friction, as well as chemical inertness and excellent thermal stability. In contrast to graphite and diamond, two crystalline forms of C, in which all C atoms have either the sp^2 , three-fold (graphite) or the sp^3 , four-fold (diamond) bonding configuration, a-C is a mixture of sp^2 and sp^3 -bonded C atoms. Conventional amorphous carbon (a-C) prepared by evaporation or sputtering consists mostly of sp^2 -bonded C atoms⁵. In contrast, ta-C films contain a large fraction (up to $\sim 75\text{-}85\%$) of sp^3 -bonded C atoms and are synthesized using a variety of energetic-beam methods⁶ including filtered cathodic vacuum arc (FCVA), mass-separated ion beam deposition (MSIBD), and pulsed laser deposition (PLD).

The amount of sp^3 bonding in ta-C and consequently its diamond-like properties depend upon the kinetic energy (KE) of the carbon species being deposited. The early work by Pappas et al.⁷ established such a correlation for PLD. Other early experiments using FCVA, PLD, and other methods showed that films with nearly maximal sp^3 content as well as highly diamond-like properties could be produced using carbon ions whose KE ranged from ~ 20 eV to at least several hundred eV⁶. For FCVA it recently was established that the highest sp^3 fraction is obtained for C ions with KE of $\sim 80\text{-}100$ eV^{8, 9, 10}. Similarly, recent PLD experiments in our laboratory^{11, 12} show that the sp^3 -bonded fraction, film density, and optical (Tauc) band gap all reach their maximum values for incident carbon ion kinetic energies of ~ 90 eV. In this paper we summarize

the results of our previous work and also report additional data on the systematic study of changes in the bonding, optical properties, and surface morphology of PLD ta-C films as a function of the C^+ ion KE.

Recently, materials that have electronic conduction-band states with low or negative electron affinity became of great interest as they might be used for fabrication of cold cathodes for flat panel displays and similar applications. It has been established that diamond can possess a negative electron affinity surface^{13, 14} which, in principle, should allow for electron emission under very low electric fields. Unfortunately, n-doping of bulk diamond is problematic and the transport of electrons to the conduction band, required for field emission applications, is difficult to achieve. As a result, despite its low electron affinity, single crystal diamond is not a good electron emitter. Recently, a few studies of FE from ta-C were reported. The results are mixed as some researchers found ta-C to exhibit very good FE properties¹⁵ while the others^{16, 17} do not confirm these results. In this work we report the results of our investigation of field emission properties of ta-C as well as predominantly sp^2 -bonded a-C films.

2. EXPERIMENTAL

ta-C films were prepared in a high vacuum chamber with a base pressure of 3×10^{-8} Torr using a Lambda Physik Compex 301i pulsed excimer laser operated with ArF (193 nm). ArF PLD is advantageous over longer wavelengths for deposition of ta-C in that it requires lower energy fluences to produce high quality films¹². In addition, the ablated flux in ArF PLD consists mostly of monoatomic C species even at relatively low fluences¹⁸ which allows for simpler characterization of deposition conditions. Maximum laser fluences at the target were $\sim 8 \text{ J/cm}^2$ and produced C^+ KE $\sim 100 \text{ eV}$. Higher energy carbon ions were produced using a Questek 2960 excimer laser. The Questek has shorter pulse duration, higher pulse energy, and a sharply peaked beam profile which allowed C^+ ions to be produced with kinetic energies up to 225 eV. 2.54-cm diameter pyrolytic graphite targets containing $< 10 \text{ ppm}$ total impurities (Specialty Minerals, Inc., Easton, PA) were used. The substrates were kept at room temperature and placed at variable distances (4.8–7.3 cm) from the target. Typical deposition rates were 0.03–0.1 $\text{\AA}/\text{shot}$. An ion probe¹⁹ was used to determine the kinetic energy of ablated C^+ ions. It consisted of a bare coaxial-cable tip biased at -100 V and mounted on an arm that rotated it in an arc passing through the center of the ablation plume. The time corresponding to the ion current peak ("icp") was used to calculate a velocity and corresponding kinetic energy of C ions, KE_{icp} .

For spectroscopic ellipsometry (SE) and atomic force microscopy (AFM) measurements ~ 70 –200 nm thick ta-C films were deposited on p- and n-type (001)-oriented Si wafers. Surface roughness studies were carried out using a Nanoscope III AFM (Digital Instruments). A tapping rather than contact mode AFM was utilized because SiN tips used for contact-mode measurements are quickly damaged by the extreme hardness of ta-C films, resulting in degraded image quality. The SE measurements were made using the two-modulator generalized ellipsometer (2-MGE)²⁰ operating from 250 to 850 nm. The SE results were fit using a 5-medium model consisting of air/ surface roughness/ ta-C film/ interface/ Si, where the optical properties of ta-C films were modeled using the 5-parameter Tauc-Lorentz (TL) formulation for the optical functions of amorphous materials²¹. Previous studies²² have shown that this model fits SE data taken on a wide range of amorphous materials, yielding the thickness of each layer, the Tauc (optical) band gap, and the optical functions of the film.

For EELS measurements ta-C was deposited on freshly cleaved NaCl substrates which were subsequently dissolved in DI water and the resultant free-standing ta-C films were placed on folding Ni TEM grids. The thickness of the films was $\sim 30 \text{ nm}$ which is substantially lower than the mean free path for 100 keV electrons ($> 50 \text{ nm}$). In this case the effect of multiple scattering can be neglected. The EELS measurements were carried out using a VG HB501 STEM fitted with a high sensitivity parallel EELS and operated at 100 keV. The energy resolution was 1.1 eV during the measurements, as determined by the FWHM of the zero-loss peak. We did not observe any notable degradation or contamination of the specimens throughout the experiments.

Field emission measurements were carried out in a high vacuum chamber with a base pressure of 10^{-6} Torr. The measurements were taken by applying a positive voltage to a tungsten-carbide current probe (anode) with tip diameter of $\sim 25 \mu\text{m}$ and by collecting electrons emitted from the samples tested (cathode). The current probe stage motion was computer controlled with the minimum step size of 75 nm in x-y-z directions, which allowed for precise control of the distance between the probe and the sample.

3. RESULTS AND DISCUSSION

3.1 EELS and ellipsometry measurements of sp^3 fraction, film density, and optical band gap

The K-edge spectra of ta-C films deposited by ArF PLD with various C^+ ion kinetic energies (KE_{icp}) corresponding to the ion current peak at the ion probe are shown in Fig. 1a. The spectra exhibit two main features: a peak at ~ 285 eV and a broad band with a maximum at ~ 293 eV. These features are due to $1s-\pi^*$ and $1s-\sigma^*$ electronic transitions, respectively²³. The former is associated with sp^2 -bonded C atoms and the latter with both sp^2 and sp^3 C atoms. One can see that the relative intensity of the $1s-\pi^*$ peak changes with the C ion KE_{icp} and becomes the lowest for the films prepared with KE_{icp} in the range of 70-120 eV. This corresponds to the materials with the lowest sp^2 content and hence more diamond-like properties.

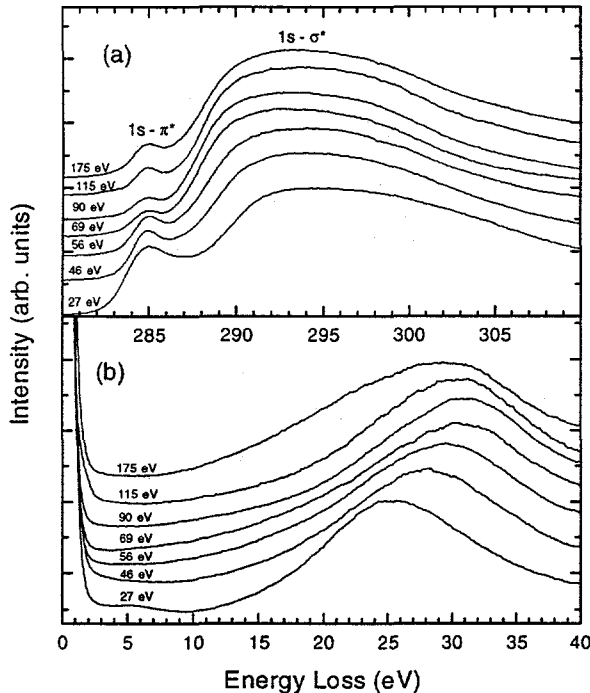


Figure 1. EELS K-edge (a) and plasmon (b) spectra of amorphous C films prepared by ArF PLD at various C ion kinetic energies (KE_{icp}) corresponding to the ion current peak of the ion probe signal.

EELS spectra also were measured in the low-energy range and are shown in Fig. 1b. The broad peak around 30 eV is associated with collective excitation, or a plasmon, of the valence electrons²³. Using a simple Drude-like model, the energy of this plasmon is proportional to the density of ta-C films²⁴: the higher the plasmon energy, the higher the film density. As two reference points one can use the plasmon peak position of graphite (~26.5 eV) and of diamond (33.6 eV).

The analysis of the sp^3 fractions in the ta-C films was performed in a way similar to that of Berger et al.²³. The sp^2 fraction, f_{sp^2} , is calculated by taking the ratio of integrated intensities of the $1s-\pi^*$ and $1s-\sigma^*$ peaks, I_π / I_σ , and by comparing it to that of arc-evaporated a-C, which is assumed to be entirely sp^2 bonded. The sp^3 fraction is then simply $1-f_{sp^2}$. There are quite a few uncertainties in the data analysis and interpretation associated with this method¹¹. In addition, the difficulty of sample preparation is also an issue for this technique. Yet, in spite of these problems, EELS is currently the most-used tool for analyzing the sp^3 fraction in ta-C. Partly this is due to the absence of any more suitable alternative method, although uv Raman scattering may be a good candidate. In contrast to conventional Raman scattering in the visible, uv Raman scattering directly reveals the presence of sp^3 -bonded C atoms^{25,26} and therefore provides a potential means of simple,

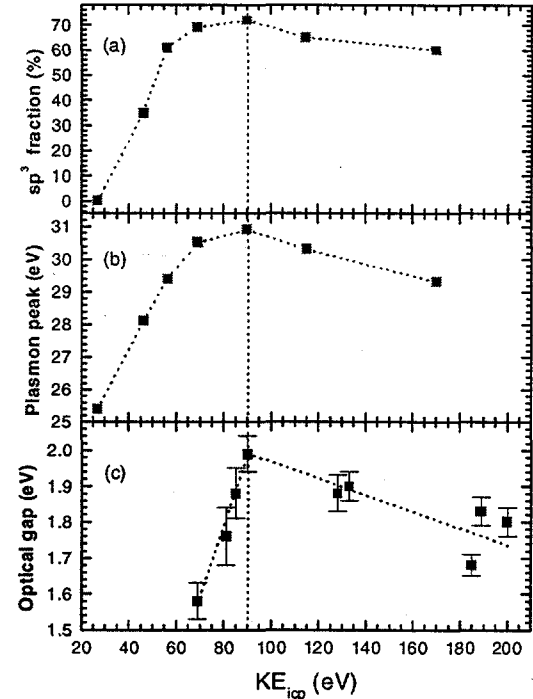


Figure 2. sp^3 content (a) and plasmon peak position (b) extracted from the EELS measurements (Fig. 1) and optical (Tauc) energy gap (c) obtained by scanning ellipsometry, as a function of C ion kinetic energy, KE_{icp} .

nondestructive characterization of ta-C films. We believe that a combination of techniques, such as EELS, ellipsometry, Raman scattering, and possibly others, is required to fully characterize such a complicated material as ta-C. Nevertheless, EELS provides a reasonable sp^3 estimate suitable for most practical applications.

Briefly, the EELS data analysis includes decomposition of the $1s-\pi^*$ and $1s-\sigma^*$ peaks via a best fit of a Gaussian into the lower energy edge of the latter. The value of I_σ was taken as an integral over the energy range of 290 - 310 eV which is large enough to avoid any significant systematic error. The extracted sp^3 fractions as a function of C ion KE_{icp} are shown in Fig. 2a. The sp^3 fraction clearly exhibits a maximum of ~ 73% at $KE_{icp} \sim 90$ eV. This is consistent with the optimum KE obtained for FCVA deposition of ta-C.

Fig. 2b shows that the position of the C plasmon peak also reaches its highest value of ~30.9 eV at $KE_{icp} \sim 90$ eV. This behavior is expected since higher plasmon peak energy corresponds to higher film density, which is characteristic of more diamond-like films with higher sp^3 content. It should be noted that the plasmon peak position can serve as a useful tool for correlating the sp^3 fractions obtained by different research groups. Inter-laboratory discrepancies in the estimate of sp^3 fractions can arise from various factors, including structural differences in sp^2 calibration samples, variations in the energy ranges and fitting procedures used to define I_π and I_σ , and differences in EELS resolution. The position of the plasmon peak is a more settled parameter and therefore can be used as a reference point for extracting the sp^3 fraction.

The EELS results were correlated with scanning ellipsometry (SE) measurements of the optical properties of ta-C films. The optical energy gaps extracted from the SE measurements are shown in Fig. 2c as a function of the C ion KE_{icp} . The trend is very similar to that observed for the sp^3 fraction and for the position of the plasmon peak. The energy gap is lower for the films prepared at low KE_{icp} , reaches its maximum at $KE_{icp} \sim 90$ eV, and decreases for higher values of KE_{icp} . This is consistent with the variation of the sp^3 fraction in these materials: sp^3 rich films are expected to have a larger optical gap (5.5 eV for pure crystalline diamond) and the gap disappears for predominantly sp^2 -bonded carbon.

3.2 Spatial variation of film thickness and optical band gap of ta-C films

Measurements of the angular distribution of the C^+ KE_{icp} also were carried out since this determines the maximum area within which spatially uniform film properties can be obtained at any given target-substrate separation, D_{ts} . As shown in Fig. 3, KE_{icp} was nearly constant ($\pm 10\%$) within a half-angular range of 12 to 15 degrees on either side of the plume centerline. At $D_{ts} = 10$ cm, for instance, this corresponds to a ~ 20 cm^2 region of uniform film properties.

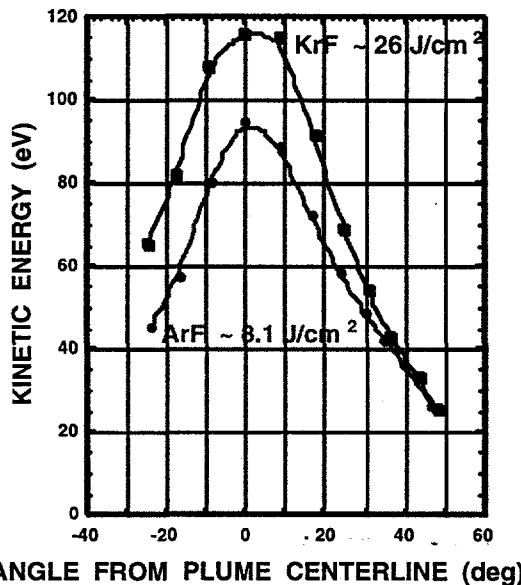


Figure 3. Angular variation of C^+ ion kinetic energy for ArF (193 nm) and KrF (248 nm) laser ablation of pyrolytic graphite.

Also, SE measurements of ta-C films deposited on 7.5 cm diameter Si wafers were employed to study film properties as a function of distance away from the plume center. It was found that not only film thickness but also the optical energy gap (E_g) varied with distance away from the plume center. This is due to the fact that diamondlike properties are a function of C ion KE which, in turn, depends on the angle from the plume centerline (see Fig. 3). If KE_{icp} at the plume center is not substantially higher than 90 eV, as shown in Fig. 4, then uniform diamond-like properties ($E_g \sim \text{constant}$) result over a large central area with properties changing rapidly only further away. However, if a much higher central KE_{icp} is used, such as in the case of $KE_{icp} = 200$ eV presented in Fig. 4, then a *degraded* central area is produced (with E_g *increasing* away from center) surrounded by a ring of the most diamond-like ta-C, with a rapid fall-off in properties still further away. These angular dependences of E_g are consistent with the energy dependence shown in Fig. 2c and the angular distribution of KE_{icp} in Fig. 3 and again confirm the existence of the optimum KE_{icp} of ~ 90 eV for ta-C film deposition.

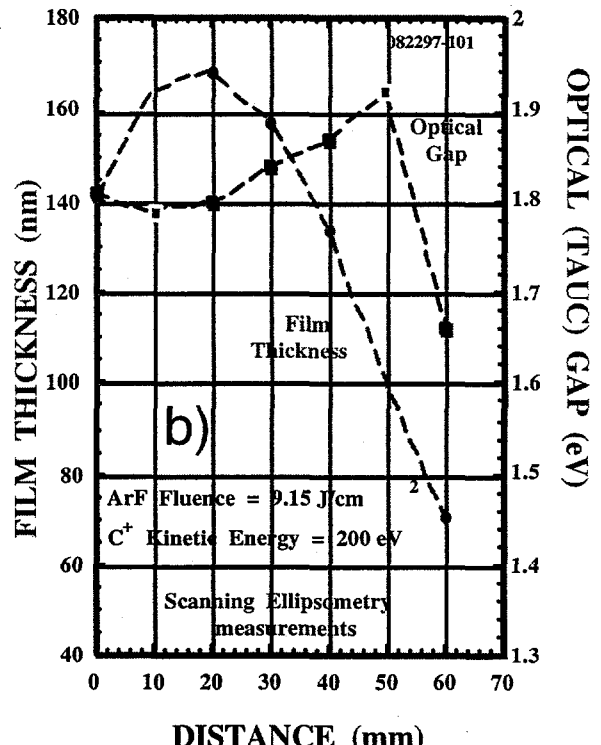
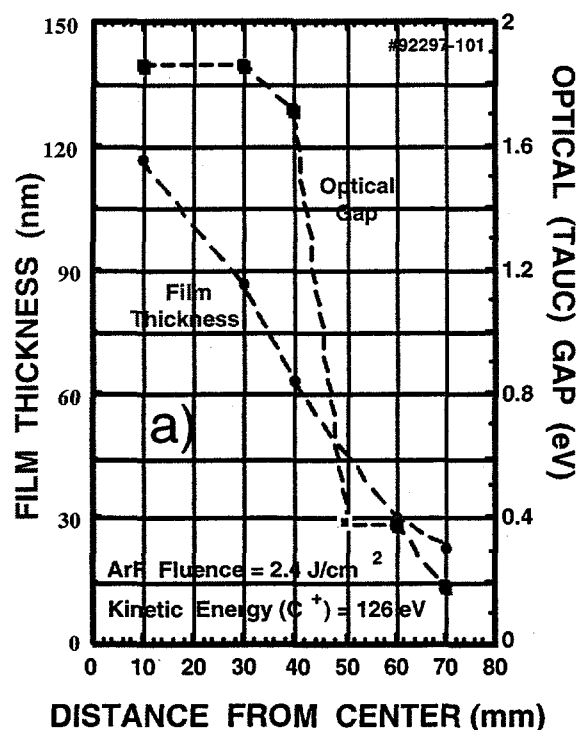


Figure 4. Spatial variation of film thickness and optical (Tauc) energy gap in a ta-C film deposited at the plume-center KE_{icp} of 126 eV (a) and 200 eV (b).

3.3 AFM studies of surface roughness of ta-C films

The AFM images shown in Fig. 5 reveal that ta-C films deposited at KE_{icp} values of 26, 44, and 90 eV all are quite smooth but still display systematic differences in roughness that are correlated with the KE_{icp} of the C ions used for deposition. Films deposited at 90 eV are extremely smooth with an rms roughness of ~ 0.9 Å measured over $(200 \text{ nm})^2$ areas. For 26 and 44 eV the corresponding rms roughness values are ~ 1.6 Å. Similarly, the Z-range of height variation within the $(200 \text{ nm})^2$ area increases from ~ 0.9 Å (at 90 eV) to ~ 1.6 Å (at 26 eV). We note that these energetically deposited carbon films also are relatively free of the large ($\sim \mu\text{m}$ scale) particulates sometimes produced by pulsed laser deposition, with typical and largest particulate diameters of $\sim 2\text{--}10$ nm and ~ 100 nm, respectively.

The tapping mode (TM) AFM results of Fig. 5 are in good agreement with the AFM measurements reported by Lifshitz⁶ for ta-C films deposited on silicon substrates by the MSIBD method. Lifshitz found a pronounced increase in roughness for films deposited at a C ion kinetic energy of 10 eV but very smooth films for kinetic energies ranging from 50 eV up to 10 keV.

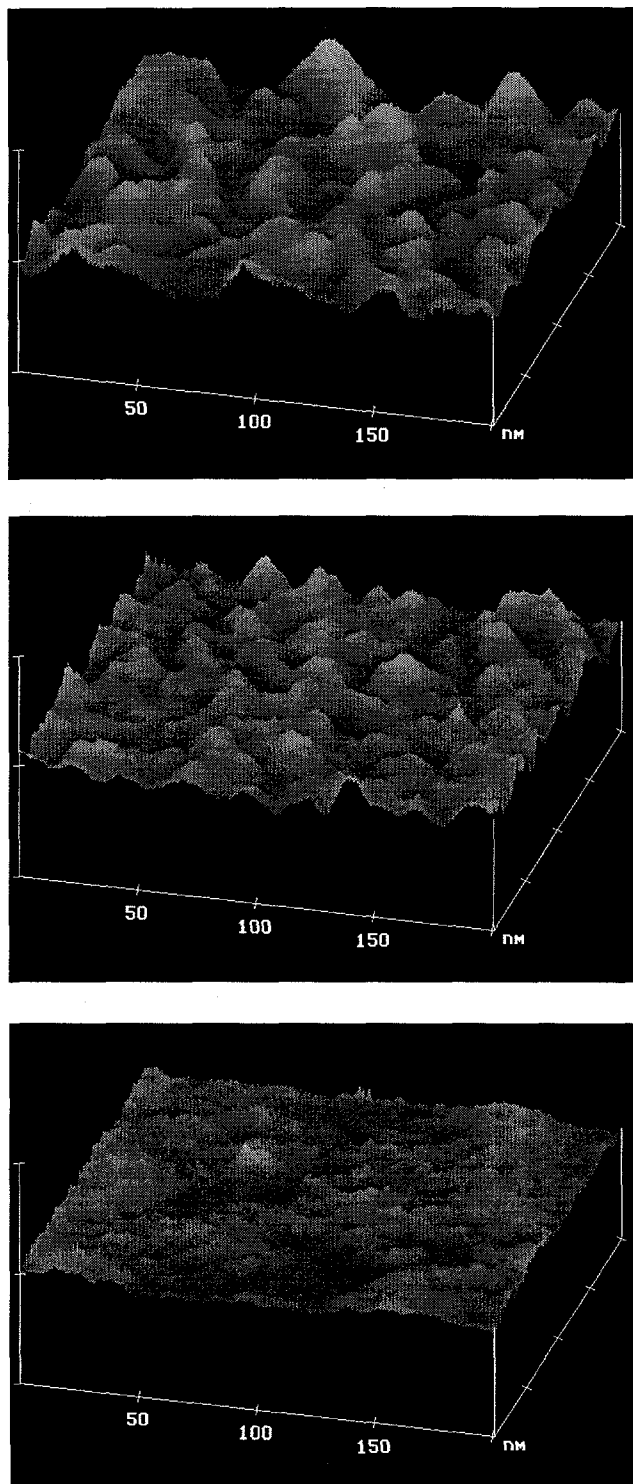


Figure 5. TM-AFM images of the surfaces of amorphous carbon films deposited at kinetic energies (KE_{icp}) of (top) 26 eV, (middle) 44 eV, and (bottom) 90 eV. [z range = 2 nm]

3.4 Field emission properties of amorphous carbon films

The emission current-applied electric field (I-E) measurements were done at a fixed distance between the probe and the sample and are shown in Fig. 6. The macroscopic electric field, E , was simply calculated as the probe voltage divided by the probe-sample distance. A typical turn-on voltage required to draw field emission current of $\sim 1\text{nA}$ from highly sp^3 -bonded C films was found to be $\sim 50\text{ V}/\mu\text{m}$. This is substantially higher than that obtained for other forms of carbon materials, such as nanostructured C films¹⁷, CVD diamond²⁷, nanodiamond²⁸, and carbon nanotubes²⁹. In fact, conventional, predominantly sp^2 -bonded a-C prepared by PLD with low C ion kinetic energies exhibits very similar field emission characteristics, with even lower fluctuations of the emission current (see Fig. 6b). The emission curves follow the Fowler-Nordheim (FN) behavior as shown in the insets of Fig. 6a and 6b. Using a simplified FN equation³⁰ and assuming the work function of graphite ($\Phi = 4.6\text{ eV}$) for amorphous C films, it is possible to estimate the emission area (EA) and the geometric enhancement factor (β) of the electric field due to sample's surface morphology. The calculations yield high $\beta \sim 100-150$ and low EA $\sim 10^{-2}\text{ }\mu\text{m}^2$ for both ta-C and sp^2 -bonded a-C films.

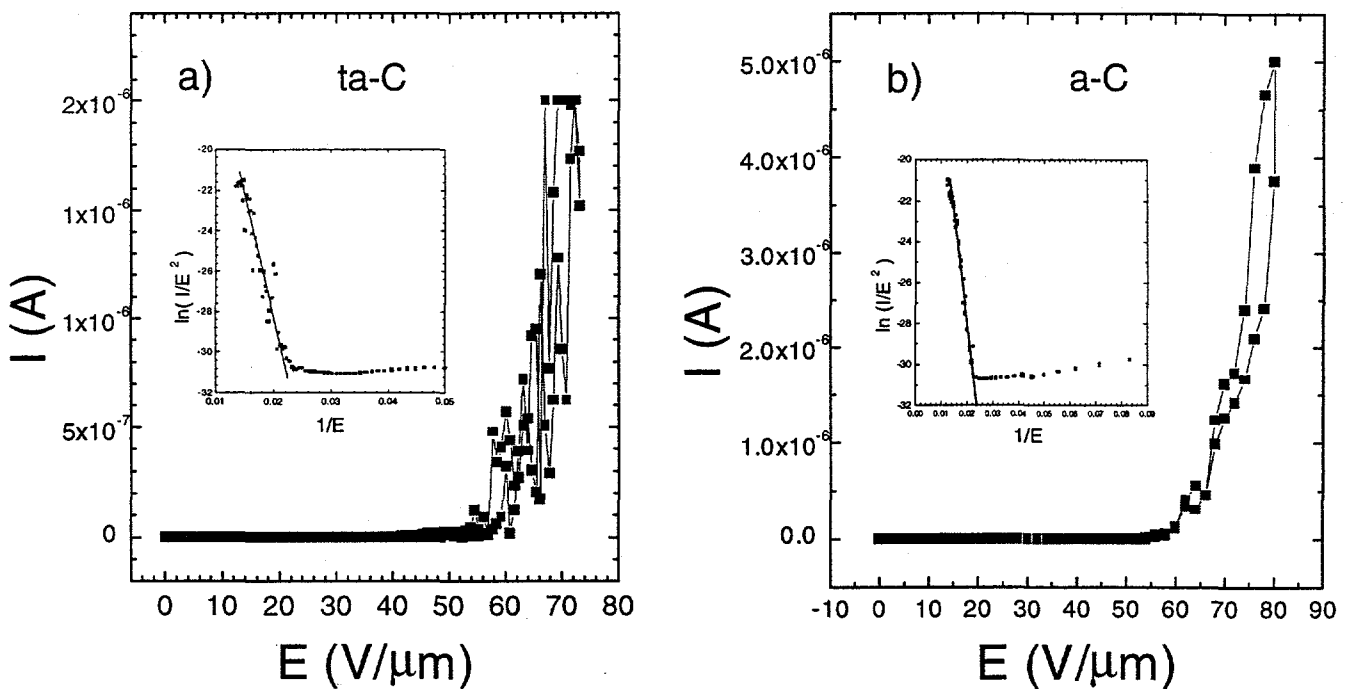


Figure 6. Emission current-applied electric field (I-E) curves and Fowler-Nordheim plots (insets) for 73% sp^3 ta-C (a) and predominantly sp^2 a-C (b) films.

Also, it has to be noted that “conditioning” was required to obtain emission from all samples tested. The conditioning typically resulted in arcing occurred between the probe and the sample as the electric field was increased from 0 to 100-200 $\text{V}/\mu\text{m}$. SEM was employed to study changes in surface morphology that occurred after the arcing. It was found that at the location where the arcing had taken place a crater of once-molten C film and Si substrate formed (see Fig. 7). Given this fact and the FE characteristics of ta-C films described above, we conclude that FE from ta-C is not due to its low electron affinity but rather should be attributed to the sharp protrusions around the crater formed during the arcing. The protrusions geometrically enhance the electric field around them, thereby providing for electron emission at moderate fields. These results are in good agreement with the observations of Talin et al.¹⁶, Coll et al.¹⁷ and Groning et al.³¹ but differ from that obtained by Satyanarayana et al¹⁵. However, the latter used parallel plate anode geometry in their experiments. This method has a drawback of “picking-up” the hottest spot on the sample and therefore provides no reliable information about the

average FE properties of the material over large surface areas. Also, in this method the leakage current across the spacers separating the anode from the cathode (sample) is rather difficult to distinguish from the true FE current.

Finally, stability tests of FE from ta-C films were performed and a representative run is shown in Fig. 8. We have found the FE to be typically quite unstable and stop after a few minutes of operation. This can be attributed to the fact of the emission sites being quite sharp. As a result, they draw extremely high current densities and consequently burn out rather quickly. In addition, rather poor vacuum of 10^{-6} Torr may also be an issue as the ion bombardment during the FE measurements may severely damage and consequently terminate the emitting sites.

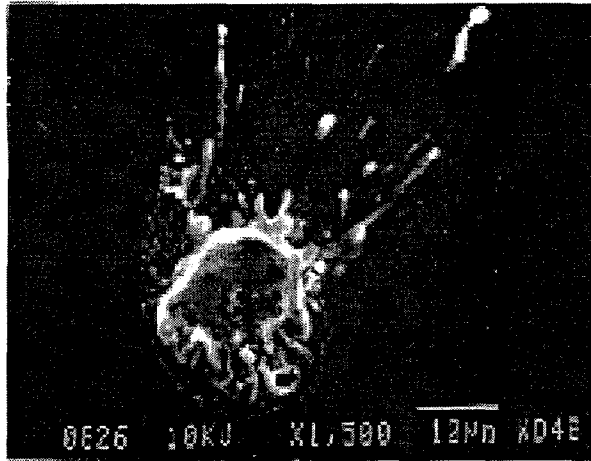


Figure 7. SEM image of a crater formed as a result of the conditioning process (arc discharge) of amorphous C films.

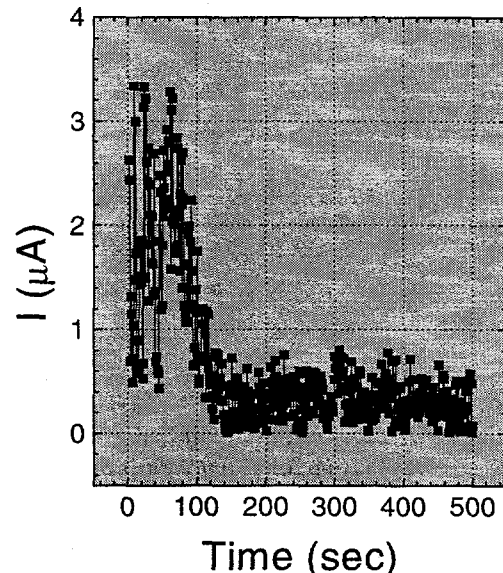


Figure 8. Instability of field emission from ta-C films.

SUMMARY AND CONCLUSIONS

In conclusion, the combination of ArF pulsed laser deposition and in situ ion probe measurements allows for deposition of ta-C films with well-controlled diamond-like properties. EELS measurements show that both the sp^3 fraction and the plasmon peak energy (\sim film density) reach their maximum values of $\sim 73\%$ and 30.9 eV in films deposited at $KE_{icp} \sim 90$ eV. Scanning ellipsometry measurements reveal that the optical (Tauc) energy gap is also maximized (~ 2.0 eV) at $KE_{icp} \sim 90$ eV, consistent with the presence of the highest sp^3 fraction. This combination of independent optical and electronic measurements provides strong evidence of an optimum kinetic energy $KE_{icp} \sim 90$ eV for ArF PLD of ta-C. Measurements of the angular distribution of C^+ kinetic energy show that films with highly uniform ($\pm 10\%$) diamond-like properties are obtained within a half-angular range of at least 12–15 degrees on either side of the plume centerline. Tapping-mode AFM measurements show that films deposited at near-optimum KE are extremely smooth, with rms roughness of only ~ 1 Å over distances of several hundred nm, and are relatively free of particulates. A distinct increase of surface roughness is observed with decreasing C^+ ion KE and is associated with the increase in sp^2 -bonding fraction. Finally, field emission measurements reveal that ta-C does not possess low electron affinity and consequently exhibits rather poor field emission characteristics (high turn-on voltages, strong current fluctuations, short life-time). However, we believe that other kinds of C-based materials, such as nanodiamond, nanotubes, and nanostructured C films, are exceptionally good candidates for various FE applications.

ACKNOWLEDGMENTS

The authors thank S. J. Pennycook for making available the STEM with which the EELS measurements were carried out and P. H. Fleming for assistance with sample preparation. This research was partially sponsored by the Defense Advanced Research Projects Agency under contract DARPA-MIPR-97-1357 with Oak Ridge National Laboratory (ORNL), and by the Office of Basic Energy Sciences, Division of Materials Sciences, U. S. Department of Energy. The research was carried out at ORNL, managed by Lockheed Martin Energy Research Corp. for the U. S. Department of Energy, under contract DE-AC05-96OR22464.

REFERENCES

1. S. Aisenberg and R. Chabot, *J. Appl. Phys.* **42**, 2953 (1971).
2. I. I. Aksenov, V. A. Belous, V. G. Podalka, and V. M. Khoroshikh, *Sov. J. Plasma Phys.* **4**, 425 (1978).
3. J. Robertson, *Prog. Solid State Chem.* **21**, 199 (1991).
4. D. R. McKenzie, Y. Yin, N. A. Marks, C. A. Davis, E. Kravtchinskaia, B. A. Pailthorpe, G. A. J. Amaratunga, *J. Non-Crystalline Solids* **164-166**, 1101 (1993).
5. H. Pan, M. Pruski, B. C. Gerstain, F. Li, and J. S. Lannin, *Phys. Rev. B* **44**, 6741 (1991).
6. Y. Lifshitz, *Diamond Relat. Mater.* **5**, 388 (1996).
7. D. L. Pappas, K. L. Saenger, J. J. Cuomo, and R. W. Dreyfus, *J. Appl. Phys.* **72**, 3966 (1992).
8. S. Ravi, P. Silva, S. Xu, B. X. Tay, H. S. Tan, and W. I. Milne, *Appl. Phys. Lett.* **69**, 491 (1996).
9. S. R. P. Silva, S. Xu, B. K. Tay, H. S. Tan, H.-J. Scheibe, M. Chhowalla, and W. I. Milne, *Thin Solid Films* **290-291**, 317 (1996).
10. M. Chhowalla, J. Robertson, C. W. Chen, S. R. P. Silva, C. A. Davis, G. A. J. Amaratunga, and W. I. Milne, *J. Appl. Phys.* **81**, 139 (1997).
11. V. I. Merkulov, D. H. Lowndes, G. E. Jellison, Jr., A. A. Puretzky, and D. B. Geohegan, *Appl. Phys. Lett.* **73**, 2591 (1998).
12. D. H. Lowndes, V. I. Merkulov, A. A. Puretzky, D. B. Geohegan, G. E. Jellison, Jr., C. M. Rouleau, and T. Thundat, p. 325 in *Advances in Laser Ablation of Materials* (ed. by R. Singh et al.), Materials Research Society, Warrendale (1998).
13. F. J. Himpel, J. A. Knapp, J. A. Van Vechten, D. E. Eastman, *Phys. Rev. B* **20**, 624 (1979).
14. J. Van der Weide and R. J. Nemanich, *Appl. Phys. Lett.* **62**, 1878 (1993).
15. B. S. Satyanarayana, A. Hart, W. I. Milne, and J. Robertson, *Appl. Phys. Lett.* **71**, 1430 (1997).
16. A. A. Talin, T. E. Felter, T. A. Friedmann, J. P. Sullivan, and M. P. Siegal, *J. Vac. Sci. Tech. A* **14**, 1719 (1996).
17. B. F. Coll, J. E. Jaskie, J. L. Markham, E. P. Menu, A. A. Talin, P. von All, p. 185 in *Covalently Bonded Disordered Thin-Film Materials* (ed. by M. P. Siegal et al.), Materials Research Society, Warrendale (1998).
18. A. A. Puretzky, D. B. Geohegan, G. E. Jellison, M. M. McGibbon, *Appl. Surf. Sci.* **96-98**, 859 (1996).
19. D. B. Geohegan, p. 124-127 and p. 147-8 in *Pulsed Laser Deposition of Thin Films* (ed. by D. B. Chrisey and G. K. Hubler), John Wiley & Sons, New York, 1994.
20. G. E. Jellison, Jr., and F. A. Modine, *Appl. Opt.* **36**, 8184 (1997); G. E. Jellison, Jr., and F. A. Modine, *Appl. Opt.* **36**, 8190 (1997).
21. G. E. Jellison, Jr., and F. A. Modine, *Appl. Phys. Lett.* **69**, 371 (1996); G. E. Jellison, Jr., and F. A. Modine, *Appl. Phys. Lett.* **69**, 2137 (1996).
22. G. E. Jellison, Jr., D. B. Geohegan, D. H. Lowndes, A. A. Puretzky, and V. I. Merkulov, p. 349 in *Advances in Laser Ablation of Materials* (ed. by R. Singh et al.), Materials Research Society, Warrendale (1998); G. E. Jellison, Jr., F. A. Modine, P. Doshi, and A. Rohatgi, *Thin Solid Films* **313-314**, 193 (1998).
23. S. D. Berger and D. R. McKenzie, and P. J. Martin, *Phil. Mag. Lett.* **57**, 285 (1988).
24. R. F. Egerton, *Electron Energy Loss Spectroscopy in the Electron Microscope* (Plenum, NY, 1986).
25. V. I. Merkulov, J. S. Lannin, C. H. Munro, S. A. Asher, V. S. Veerasamy, and W. I. Milne, *Phys. Rev. Lett.* **78**, 4869 (1997).
26. K. W. R. Gilkes, H. S. Sands, D. N. Batchelder, J. Robertson, and W. I. Milne, *Appl. Phys. Lett.* **70**, 1980 (1997).
27. D. Zhou, A. R. Krauss, T. D. Corrigan, T. G. McCauley, R. P. H. Chang, and D. M. Gruen, *J. Electrochem. Soc.* **144**, 224 (1997).
28. W. Zhu, G. P. Kochanski, S. Jin, *Science* **282**, 1471 (1998).
29. W. A. de Heer, A. Chatelain, and D. Ugarte, *Science* **270**, 1179 (1995).

30. C. A. Spindt, I. Brodie, L. Humphrey, and E. R. Westerberg, *J. Appl. Phys.* **47**, 5248 (1976).
31. O. Groning, O. M. Kuttel, E. Schaller, P. Groning, and L. Schlapbach, *Appl. Phys. Lett.* **69**, 476 (1996).